

# Quasinormal Modes of AdS Black Holes and the Approach to Thermal Equilibrium

GARY T. HOROWITZ AND VERONIKA E. HUBENY

*Physics Department, University of California, Santa Barbara, CA 93106, USA*

## Abstract

We investigate the decay of a scalar field outside a Schwarzschild anti de Sitter black hole. This is determined by computing the complex frequencies associated with quasinormal modes. There are qualitative differences from the asymptotically flat case, even in the limit of small black holes. In particular, for a given angular dependence, the decay is always exponential - there are no power law tails at late times. In terms of the AdS/CFT correspondence, a large black hole corresponds to an approximately thermal state in the field theory, and the decay of the scalar field corresponds to the decay of a perturbation of this state. Thus one obtains the timescale for the approach to thermal equilibrium. We compute these timescales for the strongly coupled field theories in three, four, and six dimensions which are dual to string theory in asymptotically AdS spacetimes.

September, 1999

## 1. Introduction

It is well known that if you perturb a black hole, the surrounding geometry will “ring”, i.e., undergo damped oscillations. The frequencies and damping times of these oscillations are entirely fixed by the black hole, and are independent of the initial perturbation. These oscillations are similar to normal modes of a closed system. However, since the field can fall into the black hole or radiate to infinity, the modes decay and the corresponding frequencies are complex. These oscillations are known as “quasinormal modes”. For black holes in asymptotically flat spacetimes, they have been studied for almost thirty years [1,2]. The radiation associated with these modes is expected to be seen with gravitational wave detectors in the coming decade. Motivated by inflation, the quasinormal modes of black holes in de Sitter space have recently been studied [3,4].

For spacetimes which asymptotically approach anti de Sitter (AdS) spacetime the situation is slightly different. In the absence of a black hole, most fields propagating in AdS can be expanded in ordinary normal modes. The cosmological constant provides an effective confining box, and solutions only exist with discrete (real) frequencies. However once a black hole is present, this is no longer the case. The fields can now fall into the black hole and decay. There should exist complex frequencies, characteristic of the black hole, which describe the decay of perturbations outside the horizon. We will compute these quasinormal frequencies below, for spacetimes of various dimensions.

The quasinormal frequencies of AdS black holes have a direct interpretation in terms of the dual conformal field theory (CFT) [5,6,7,8].<sup>1</sup> According to the AdS/CFT correspondence, a large static black hole in AdS corresponds to an (approximately) thermal state in the CFT. Perturbing the black hole corresponds to perturbing this thermal state, and the decay of the perturbation describes the return to thermal equilibrium. So we obtain a prediction for the thermalization timescale in the strongly coupled CFT. It seems difficult to compute this timescale directly in the CFT. Since the system will clearly not thermalize in the free field limit, at weak coupling, this timescale will be very long and depend on the coupling constant. In the limit of strong coupling, it seems plausible that the timescale will remain nonzero, and be independent of the coupling. This is because

---

<sup>1</sup> The importance of these modes in AdS was independently recognized in [9], but they were not computed. They were computed in [10], but only for a conformally invariant scalar field whose asymptotic behavior is similar to flat spacetime. The confining behavior of AdS is crucial for the AdS/CFT correspondence.

the initial state is characterized by excitations with size of order the thermal wavelength, so causality suggests that the relaxation timescale should also be of order the thermal wavelength.

The results we obtain are consistent with this expectation. A black hole in AdS is determined by two dimensionful parameters, the AdS radius  $R$  and the black hole radius  $r_+$ . The quasinormal frequencies must be functions of these parameters. For large black holes,  $r_+ \gg R$ , we will show that there is an additional symmetry which insures that the frequencies can depend only on the black hole temperature  $T \sim r_+/R^2$ . However, for smaller black holes, this is no longer the case. Whereas the temperature begins to increase as one decreases  $r_+$  below  $R$ , we find that the (imaginary part of the) frequency continues to decrease with  $r_+$ . This is different from what happens for asymptotically flat black holes. An ordinary Schwarzschild black hole has only one dimensionful parameter which can be taken to be the temperature. Its quasinormal frequencies must therefore be multiples of this temperature. Thus small black holes in AdS do NOT behave like black holes in asymptotically flat spacetime. The reason is simply that the boundary conditions at infinity are changed. More physically, the late time behavior of the field is affected by waves bouncing off the potential at large  $r$ .

Another difference from the asymptotically flat case concerns the decay at very late times. For a Schwarzschild black hole, it is known that the exponential decay associated with the quasinormal modes eventually gives way to a power law tail [11]. This has been shown to be associated with the scattering of the field off the Coulomb potential at large  $r$ . As we will discuss later, for asymptotically AdS black holes, this does not occur.

We will compute the quasinormal frequencies for Schwarzschild-AdS black holes in the dimensions of interest for the AdS/CFT correspondence: four, five, and seven. We will consider minimally coupled scalar perturbations representing, e.g., the dilaton. This corresponds to a particular perturbation of the CFT. For example, for  $AdS_5$ , it corresponds to a perturbation of an (approximately) thermal state in super Yang-Mills on  $S^3 \times R$  with  $\langle F^2 \rangle$  nonzero. In the linearized approximation we are using, the spacetime metric is not affected by the scalar field. So the perturbation of the thermal state does not change the energy density, which remains uniform over the sphere. The late time decay of this perturbation is universal in the sense that all solutions for the dilaton with the same angular dependence will decay at the same rate, which is determined by the imaginary part of the lowest quasinormal frequency. Different perturbations, corresponding to different lin-

earized supergravity fields, will have different quasinormal frequencies and hence decay at different rates. Although we work in the classical supergravity limit, our results would not be affected if one includes small semiclassical corrections such as black holes in equilibrium with their Hawking radiation.

A brief outline of this paper is the following. In the next section we review the definition of quasinormal modes, their relation to the late time behavior of the field, and derive some of their properties using analytic arguments. The numerical approach we use to compute the complex frequencies is described in section 3. In the following section we discuss the results for both large black holes  $r_+ \gg R$  and intermediate size black holes  $r_+ \sim R$ . In section 5 we consider the limit of small black holes  $r_+ \ll R$ . Although there is a striking similarity between some of our results and some results obtained in the study of black hole critical phenomena [12], we will argue that this is probably just a numerical coincidence. The conclusion contains some speculations about the CFT interpretation of the quasinormal frequencies in the regime where they do not scale with the temperature. In the appendix, we give some more details on our numerical calculations.

## 2. Definition of quasinormal modes and analytic arguments

Since we are interested in studying AdS black holes in various dimensions, we begin with the  $d$  dimensional Schwarzschild-AdS metric:

$$ds^2 = -f(r) dt^2 + f(r)^{-1} dr^2 + r^2 d\Omega_{d-2}^2 \quad (2.1)$$

where

$$f(r) \equiv \frac{r^2}{R^2} + 1 - \left(\frac{r_0}{r}\right)^{d-3}. \quad (2.2)$$

$R$  is the AdS radius and  $r_0$  is related to the black hole mass via

$$M = \frac{(d-2)A_{d-2} r_0^{d-3}}{16\pi G_d} \quad (2.3)$$

where  $A_{d-2} = 2\pi^{\frac{d-1}{2}}/\Gamma(\frac{d-1}{2})$  is the area of a unit  $(d-2)$ -sphere. The black hole horizon is at  $r = r_+$ , the largest zero of  $f$ , and its Hawking temperature is

$$T = \frac{f'(r_+)}{4\pi} = \frac{(d-1)r_+^2 + (d-3)R^2}{4\pi r_+ R^2} \quad (2.4)$$

We are interested in solutions to the minimally coupled scalar wave equation

$$\nabla^2 \Phi = 0 \tag{2.5}$$

If we consider modes

$$\Phi(t, r, \text{angles}) = r^{\frac{2-d}{2}} \psi(r) Y(\text{angles}) e^{-i\omega t} \tag{2.6}$$

where  $Y$  denotes the spherical harmonics on  $S^{d-2}$ , and introduce a new radial coordinate  $dr_* = dr/f(r)$ , the wave equation reduces to the standard form

$$[\partial_{r_*}^2 + \omega^2 - \tilde{V}(r_*)] \psi = 0. \tag{2.7}$$

The potential  $\tilde{V}$  is positive and vanishes at the horizon, which corresponds to  $r_* = -\infty$ . It diverges at  $r = \infty$ , which corresponds to a finite value of  $r_*$ .

To define quasinormal modes, let us first consider the case of a simple Schwarzschild black hole. Since the spacetime is asymptotically flat, the potential now vanishes near infinity. Clearly, a solution exists for each  $\omega$  corresponding to a wave coming in from infinity, scattering off the potential and being partly reflected and partly absorbed by the black hole. Quasinormal modes are defined as solutions which are purely outgoing near infinity  $\Phi \sim e^{-i\omega(t-r_*)}$  and purely ingoing near the horizon  $\Phi \sim e^{-i\omega(t+r_*)}$ . No initial incoming wave from infinity is allowed. This will only be possible for a discrete set of complex  $\omega$  called the quasinormal frequencies.

For the asymptotically AdS case, the potential diverges at infinity, so we must require that  $\Phi$  vanish there. In the absence of a black hole,  $r_*$  has only a finite range and solutions exist for only a discrete set of real  $\omega$ . However once the black hole is added, there are again solutions with any value of  $\omega$ . These correspond to an outgoing wave coming from the (past) horizon, scattering off the potential and becoming an ingoing wave entering the (future) horizon. Quasinormal modes are defined to be modes with only ingoing waves near the horizon. These again exist for only a discrete set of complex  $\omega$ .

It should perhaps be emphasized that these modes are not the same as the ones that have recently been computed in connection with the glueball masses [13]. There are several differences: First, the background for the glueball mass calculation is not the spherically symmetric AdS black hole, but an analytic continuation of the plane symmetric AdS black hole. Second, because of the analytic continuation, the horizon becomes a regular origin, and the boundary conditions there are not the analytic continuation of the ingoing wave

boundary condition imposed for quasinormal modes. Finally, the glueball masses are real quantities, while as we have said, the quasinormal frequencies will be complex. This makes them more difficult to compute numerically.

One can show [14,2] that the complex quasinormal frequencies determine the fall off of the field at late times. The basic idea is to start by writing the solution to the wave equation in terms of the retarded Green's function and initial data on a constant  $t$  surface. One then rewrites the Green's function in terms of its Fourier transform with respect to  $t$ . The quasinormal modes arise as poles of the Green's function in the complex frequency plane, and their contributions to the solution can be extracted by closing the contour with a large semicircle near infinity.

For a black hole in asymptotically flat spacetimes, Price [11] showed that after the exponential decay due to the quasinormal ringing, the field will decay as a power law  $\Phi \sim t^{-(2l+3)}$  where  $l$  is the angular quantum number. This has been seen explicitly in numerical simulations [15]. Mathematically, this is due to a cut in the Green's function along the negative imaginary frequency axis. More physically, this behavior is due to scattering off the weak Coulomb potential near infinity. For the case of a black hole in AdS, the potential diverges at infinity and vanishes exponentially near the horizon. Ching et. al. [14] have analyzed the late time behavior of a broad class of wave equations with potentials. They show that there are no power law tails for a potential which vanishes exponentially. So there will be no power law tails for black holes in AdS.

For a black hole with radius much smaller than the AdS radius, one might expect an intermediate time regime where one sees power law behavior before the new boundary conditions at infinity become important. However, this would occur only if one starts with large quasinormal modes with  $\omega \sim 1/r_+$  associated with a Schwarzschild black hole. We will see that the lowest modes of a Schwarzschild-AdS black hole are much smaller and their exponential decay is so slow that it eliminates the intermediate time power law behavior.

The quasinormal frequencies will in general depend on the two parameters in the problem  $R, r_0$ . By rescaling the metric,  $\hat{ds}^2 = \lambda^2 ds^2$ , and rescaling the coordinates  $\hat{t} = \lambda t$  and  $\hat{r} = \lambda r$ , the new metric again takes the form (2.1) with rescaled constants  $R$  and  $r_0$ . Since the wave equation (2.5) is clearly invariant under this constant rescaling of the metric, we can use it to set e.g.  $R = 1$ . This rescaling is possible for any metric and physically just corresponds to a choice of units. In our case, we measure all quantities in

units of the AdS radius. The quasinormal frequencies can still be arbitrary functions of  $r_0$ .

We now show that for large black holes,  $r_0 \gg R$ , the frequencies must be proportional to the black hole temperature. This is a result of an independent scaling one can do in this limit. For large black holes, the region outside the horizon of the Schwarzschild-AdS metric (2.1) becomes approximately plane symmetric:

$$ds^2 = -h(r) dt^2 + h(r)^{-1} dr^2 + r^2 dx_i dx^i \quad (2.8)$$

where

$$h(r) \equiv \frac{r^2}{R^2} - \left(\frac{r_0}{r}\right)^{d-3}. \quad (2.9)$$

For this metric one can rescale  $r_0$  by a pure coordinate transformation:  $t = a\hat{t}$ ,  $x_i = a\hat{x}_i$ ,  $r = \hat{r}/a$  for constant  $a$ . This does not rescale the overall metric, or the AdS radius  $R$ . The horizon radius  $r_+^{d-1} = R^2 r_0^{d-3}$  gets rescaled by  $r_+ = \hat{r}_+/a$ . Of course, under this coordinate transformation of the metric, solutions of the wave equation are related by the same coordinate transformation. For solutions which are independent of  $x^i$  (the analog of the  $l = 0$  modes) we have  $e^{-i\omega(r_+)t} = e^{-i\omega(\hat{r}_+)\hat{t}}$ , which implies  $\omega(r_+) \propto r_+$ . Since the Hawking temperature of the metric (2.8) is also proportional to the horizon radius,

$$T = \frac{d-1}{4\pi} \frac{r_+}{R^2} \quad (2.10)$$

we see that the frequencies must scale with the temperature for large black holes. For solutions proportional to  $e^{ik_i x^i}$ , this scaling argument implies  $\omega(ar_+, ak_i) = a\omega(r_+, k_i)$ . So if  $r_+^2 \gg k_i k^i$ , one can rescale so that  $k^2$  is negligibly small. The above argument then shows that  $\omega$  still scales with the temperature. One can then rescale back to  $r_+ \gg R$  to apply to large black holes. In other words, for any  $k_i$ , the quasinormal frequencies scale with the temperature in the limit of large temperatures  $T^2 \gg k^2$ . This argument does not apply to black holes of order the AdS radius, and indeed we will find that the quasinormal frequencies do not scale with the temperature in this regime. But it does confirm the expectation that the approach to thermal equilibrium in the dual field theory should depend only on the temperature (at least for large temperature).

Since we want modes which behave like  $e^{-i\omega(t+r_*)}$  near the horizon, it is convenient to set  $v = t+r_*$ , and work with ingoing Eddington coordinates. The metric for Schwarzschild-AdS in  $d$  dimensions in ingoing Eddington coordinates is

$$ds^2 = -f(r) dv^2 + 2 dv dr + r^2 d\Omega_{d-2}^2 \quad (2.11)$$

where  $f$  is again given by (2.2). The minimally-coupled scalar wave equation (2.5) may be reduced to an ordinary, second order, linear differential equation in  $r$  by the separation of variables,

$$\Phi(v, r, \text{angles}) = r^{\frac{2-d}{2}} \psi(r) Y(\text{angles}) e^{-i\omega v} \quad (2.12)$$

This yields the following radial equation for  $\psi(r)$ :

$$f(r) \frac{d^2}{dr^2} \psi(r) + [f'(r) - 2i\omega] \frac{d}{dr} \psi(r) - V(r) \psi(r) = 0, \quad (2.13)$$

with the effective potential  $V(r)$  given by ( $R = 1$ )

$$\begin{aligned} V(r) &= \frac{(d-2)(d-4)}{4r^2} f(r) + \frac{d-2}{2r} f'(r) + \frac{c}{r^2} \\ &= \frac{d(d-2)}{4} + \frac{(d-2)(d-4) + 4c}{4r^2} + \frac{(d-2)^2 r_0^{d-3}}{4r^{d-1}} \end{aligned} \quad (2.14)$$

where

$$c = l(l + d - 3) \quad (2.15)$$

is the eigenvalue of the Laplacian on  $S^{d-2}$ . Note that  $V(r)$  is manifestly positive for  $d \geq 4$ .

Ingoing modes near the (future) horizon are described, of course, by a nonzero multiple of  $e^{-i\omega v}$ . Outgoing modes near the horizon can also be expressed in terms of ingoing Eddington coordinates via  $e^{-i\omega(t-r_*)} = e^{-i\omega v} e^{2i\omega r_*}$ . Since

$$r_* = \int \frac{dr}{f(r)} \approx \frac{1}{f'(r_+)} \ln(r - r_+) \quad (2.16)$$

near the horizon  $r = r_+$ , the outgoing modes behave like

$$e^{-i\omega(t-r_*)} = e^{-i\omega v} e^{2i\omega r_*} \approx e^{-i\omega v} (r - r_+)^{2i\omega/f'(r_+)} \quad (2.17)$$

Since  $v, r$  are good coordinates near the horizon, the outgoing modes are not smooth ( $C^\infty$ ) at  $r = r_+$  unless  $2i\omega/f'(r_+)$  is a positive integer. We show below that the imaginary part of  $\omega$  must be negative, so the exponent in (2.17) always has a positive real part. Thus the outgoing modes vanish near the future horizon, while the ingoing modes are nonzero there. However we also show (in the next section) that  $2i\omega/f'(r_+)$  cannot be a positive integer, so the outgoing modes are not smooth at  $r = r_+$ .

We wish to find the complex values of  $\omega$  such that (2.13) has a solution with only ingoing modes near the horizon, and vanishing at infinity. We will eliminate the outgoing



modes by first assuming the solution is smooth at  $r = r_+$ , and then showing that the allowed discrete values of  $\omega$  are such that  $2i\omega/f'(r_+)$  is not an integer. The actual values of  $\omega$  must be computed numerically, but some general properties can be seen analytically. For example, we now show that there are no solutions with  $i\omega$  pure real, and  $2i\omega < f'(r_+)$ . If  $i\omega$  were real, then the equation would be real and the solutions  $\psi$  would be real. If there were a local extremum at some point  $\tilde{r}$ , then  $\psi'(\tilde{r}) = 0$  and  $\psi''(\tilde{r})$  would have the same sign as  $\psi(\tilde{r})$ . So if  $\psi$  were positive at  $\tilde{r}$ , it would have to increase as  $r$  increased. Similarly, if it were negative, it would have to decrease. In neither case, could it approach zero asymptotically. We conclude that the solutions must monotonically approach zero. Now if  $2i\omega < f'(r_+)$ ,  $\psi'(r_+)$  has the same sign as  $\psi(r_+)$ .<sup>2</sup> So as one moves away from the horizon, the solutions move farther away from zero and hence can never reach zero asymptotically. This analytic argument only applies if  $2i\omega < f'(r_+)$ . But we will see numerically that even without this restriction, there are no solutions with  $i\omega$  pure real.

A more powerful result can be obtained as follows. Multiplying (2.13) by  $\bar{\psi}$  and integrating from  $r_+$  to  $\infty$  yields

$$\int_{r_+}^{\infty} dr \left[ \bar{\psi} \frac{d}{dr} \left( f \frac{d\psi}{dr} \right) - 2i\omega \bar{\psi} \frac{d\psi}{dr} - V \bar{\psi} \psi \right] = 0 \quad (2.18)$$

The first term can be integrated by parts without picking up a surface term since  $f(r_+) = 0$  and  $\bar{\psi}(\infty) = 0$ . This yields

$$\int_{r_+}^{\infty} dr [f|\psi'|^2 + 2i\omega \bar{\psi} \psi' + V|\psi|^2] = 0 \quad (2.19)$$

Taking the imaginary part of (2.19) yields

$$\int_{r_+}^{\infty} dr [\omega \bar{\psi} \psi' + \bar{\omega} \psi \bar{\psi}'] = 0 \quad (2.20)$$

Integrating the second term by parts yields

$$(\omega - \bar{\omega}) \int_{r_+}^{\infty} dr \bar{\psi} \psi' = \bar{\omega} |\psi(r_+)|^2 \quad (2.21)$$

---

<sup>2</sup> This is where the condition of no outgoing modes near the horizon is used. If outgoing waves were present,  $f(r)\psi''(r)$  would no longer vanish at  $r = r_+$ , and  $\psi'(r_+)$  need not have the same sign as  $\psi(r_+)$ .

Substituting this back into (2.19) we obtain the final result

$$\int_{r_+}^{\infty} dr [f|\psi'|^2 + V|\psi|^2] = -\frac{|\omega|^2|\psi(r_+)|^2}{\text{Im}\omega} \quad (2.22)$$

Since  $f$  and  $V$  are both positive definite outside the horizon, this equation clearly shows that there are no solutions with  $\text{Im } \omega > 0$ . These would correspond to unstable modes which grow exponentially in time. There are also no solutions with  $\text{Im } \omega = 0$ : All solutions must decay in time. In addition, eq. (2.22) shows that the only solution which vanishes at the horizon (and infinity) is zero everywhere. Since the equation is linear, we can always rescale  $\psi$  so that  $\psi(r_+) = 1$ .

### 3. Numerical approach to computing quasinormal modes

To compute the quasinormal modes, we will expand the solution in a power series about the horizon and impose the boundary condition that the solution vanish at infinity. In order to map the entire region of interest,  $r_+ < r < \infty$ , into a finite parameter range, we change variables to  $x = 1/r$ . In general, a power series expansion will have a radius of convergence at least as large as the distance to the nearest pole. Examining the pole structure of (2.13) in the whole complex  $r$  plane, we find  $d + 1$  regular singular points, at  $r = 0$ ,  $r = \infty$ , and at the  $d - 1$  zeros of  $f$ , one of which,  $r = r_+$  corresponds to the horizon. At least for  $d = 4, 5$  or  $7$ , if we use the variable  $x = 1/r$  and expand about the horizon,  $x_+ = 1/r_+$ , the radius of convergence will<sup>3</sup> reach to  $x = 0$ , so that we can use this expansion to consider the behavior of the solution as  $r \rightarrow \infty$ .

In terms of our new variable  $x = 1/r$ , (2.13) becomes

$$s(x) \frac{d^2}{dx^2} \psi(x) + \frac{t(x)}{x - x_+} \frac{d}{dx} \psi(x) + \frac{u(x)}{(x - x_+)^2} \psi(x) = 0 \quad (3.1)$$

where the coefficient functions are given by

$$s(x) = \frac{r_0^{d-3} x^{d+1} - x^4 - x^2}{x - x_+} = \frac{x_+^2 + 1}{x_+^{d-1}} x^d + \dots + \frac{x_+^2 + 1}{x_+^3} x^4 + \frac{1}{x_+^2} x^3 + \frac{1}{x_+} x^2 \quad (3.2)$$

$$t(x) = (d - 1) r_0^{d-3} x^d - 2x^3 - 2x^2 i\omega \quad (3.3)$$

---

<sup>3</sup> For  $d = 4$  and  $d = 5$ , one can show analytically that starting at the horizon,  $x = x_+$ , the nearest pole is indeed  $x = 0$ . For  $d = 7$  we have checked numerically that this is again the case.

$$u(x) = (x - x_+) V(x) \quad (3.4)$$

The parameter  $r_0^{d-3}$  should be viewed as a function of the horizon radius:  $r_0^{d-3} = \frac{x_+^2 + 1}{x_+^{d-1}}$ . Since  $s$ ,  $t$ , and  $u$  are all polynomials of degree  $d$  we may expand them about the horizon  $x = x_+$ :  $s(x) = \sum_{n=0}^d s_n (x - x_+)^n$ , and similarly for  $t(x)$  and  $u(x)$ . It will be useful to note that  $s_0 = 2x_+^2 \kappa$ ,  $t_0 = 2x_+^2 (\kappa - i\omega)$ , and  $u_0 = 0$ , where  $\kappa$  is the surface gravity, which is related to the black hole temperature (2.4) by

$$\kappa = \frac{f'(r_+)}{2} = 2\pi T. \quad (3.5)$$

Also, since  $s_0 \neq 0$ ,  $x = x_+$  is a regular singular point of (3.1).

To determine the behavior of the solutions near the horizon, we first set  $\psi(x) = (x - x_+)^\alpha$  and substitute into (3.1). Then to leading order we get

$$\alpha(\alpha - 1) s_0 + \alpha t_0 = 2x_+^2 \alpha (\alpha \kappa - i\omega) = 0 \quad (3.6)$$

which has two solutions  $\alpha = 0$  and  $\alpha = i\omega/\kappa$ . We see from (2.17) that these correspond precisely to the ingoing and outgoing modes near the horizon respectively. Since we want to include only the ingoing modes, we take  $\alpha = 0$ . This corresponds to looking for a solution of the form

$$\psi(x) = \sum_{n=0}^{\infty} a_n (x - x_+)^n \quad (3.7)$$

Substituting (3.7) into (3.1) and equating coefficients of  $(x - x_+)^n$  for each  $n$ , we obtain the following recursion relations<sup>4</sup> for the  $a_n$ :

$$a_n = -\frac{1}{P_n} \sum_{k=0}^{n-1} [k(k-1) s_{n-k} + k t_{n-k} + u_{n-k}] a_k \quad (3.8)$$

where

$$P_n = n(n-1) s_0 + n t_0 = 2x_+^2 n (n \kappa - i\omega) \quad (3.9)$$

Since the leading coefficient  $a_0$  is undetermined, this yields a one parameter family of solutions, as expected for a linear equation.

---

<sup>4</sup> Although the standard way of writing (3.1) is to set the coefficient of  $\psi''$  to 1 which yields simpler-looking recursion relations, the advantage of the present formulation is that since  $s(x)$ ,  $t(x)$ , and  $u(x)$  are polynomials, their analytic expansions will terminate after a finite number of terms, so that each  $a_n$  will be given in terms of a relatively small number of terms.

The solutions to (2.5) in asymptotically AdS spacetime are  $\Phi \sim \text{constant}$  and  $\Phi \sim 1/r^{d-1}$  as  $r \rightarrow \infty$ , which translates into  $\psi \sim r^{\frac{d-2}{2}}$  and  $\psi \sim r^{-d/2}$ , respectively. We are interested in normalizable modes, so we must select only solutions which satisfy  $\psi \rightarrow 0$  as  $r \rightarrow \infty$  (or  $x \rightarrow 0$ ). This means that we require (3.7) to vanish at  $x = 0$ , which is satisfied only for special (discrete) values of  $\omega$ . (For all other values of  $\omega$ , the solution will blow up,  $\psi(0) = \infty$ .) Thus in order to find the quasinormal modes, we need to find the zeros of  $\sum_{n=0}^{\infty} a_n(\omega) (-x_+)^n$  in the complex  $\omega$  plane. This is done by truncating the series after a large number of terms and computing the partial sum as a function of  $\omega$ . One can then find zeros of this partial sum, and check the accuracy by seeing how much the location of the zero changes as one goes to higher partial sums. Some details are given in the Appendix.

One can now easily show that  $2i\omega/f'(r_+) = i\omega/\kappa$  cannot be an integer. If  $\omega$  is pure imaginary and  $i\omega = \tilde{n}\kappa$  for some integer  $\tilde{n}$ , then  $P_{\tilde{n}} = 0$ . This implies an additional constraint on the coefficients  $a_k$ ,  $k = 0, \dots, \tilde{n} - 1$  which will only be satisfied if they vanish. In other words, the solution will behave like  $(x - x_+)^{\tilde{n}}$  near the horizon corresponding to a pure outgoing wave. However, since  $\psi$  now vanishes at the horizon, (2.22) implies that  $\psi$  vanishes everywhere. So there are no nontrivial solutions with  $i\omega/\kappa$  equal to an integer. As we saw in section two, this means that if one wanted to include outgoing modes near the (future) horizon, the solution would not be smooth there.

#### 4. Discussion of results

The numerical procedure described above can be applied to both large black holes ( $r_+ \gg R$ ) and intermediate size black holes ( $r_+ \sim R$ ). In this section we describe the results. We set  $R = 1$ , and decompose the quasinormal frequencies into real and imaginary parts:

$$\omega = \omega_R - i\omega_I \tag{4.1}$$

With the sign chosen in (4.1),  $\omega_I$  is positive for all quasinormal frequencies.

In Table 1., we list the values of the lowest quasinormal mode frequencies for  $l = 0$  and selected values of  $r_+$ , for the four, five, and seven dimensional Schwarzschild-AdS black holes. For large black holes, both the real and the imaginary parts of the frequency are linear functions of  $r_+$ . Since the temperature of a large black hole is  $T = (d - 1)r_+/4\pi$ , it follows that they are also linear functions of  $T$ . This is clearly shown in fig. 1 and fig. 2, where  $\omega_I$  and  $\omega_R$  respectively are plotted as a function of the temperature for the four,

	4d BH modes		5d BH modes		7d BH modes	
$r_+$	$\omega_I$	$\omega_R$	$\omega_I$	$\omega_R$	$\omega_I$	$\omega_R$
100	266.3856	184.9534	274.6655	311.9627	261.2	500.8
50	133.1933	92.4937	137.3296	156.0077	130.7	250.4
10	26.6418	18.6070	27.4457	31.3699	26.07	50.35
5	13.3255	9.4711	13.6914	15.9454	12.96	25.57
1	2.6712	2.7982	2.5547	4.5788	2.16	7.27
0.8	2.1304	2.5878	1.9676	4.1951		
0.6	1.5797	2.4316	1.3656	3.8914		
0.4	1.0064	2.3629	0.7462	3.7174		

Table 1: The lowest quasinormal mode frequency for the 4, 5, and 7 dimensional Schwarzschild-AdS black hole for some selected black hole sizes.

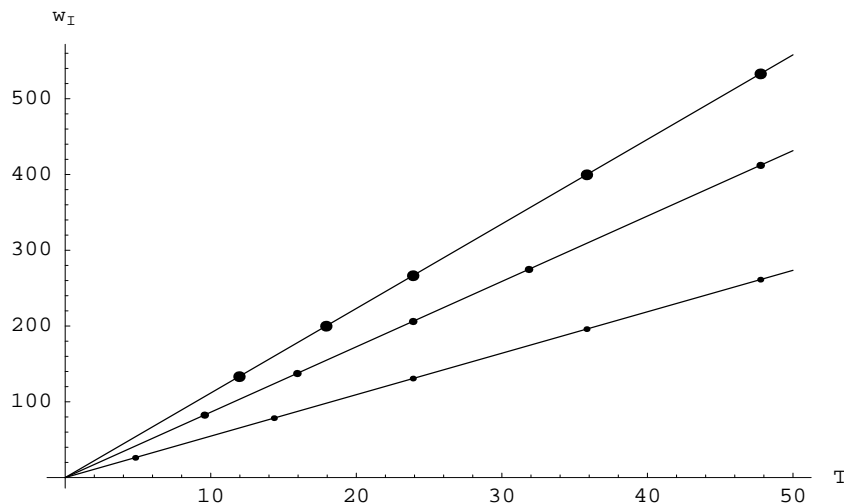


**Fig. 1:** For large black holes,  $\omega_I$  is proportional to the temperature. The top line is  $d = 4$ , the middle line is  $d = 5$  and the bottom line is  $d = 7$ .

five, and seven dimensional cases. The dots, representing the quasinormal modes, lie on straight lines through the origin. In fig. 1, the top line corresponds to the  $d = 4$  case, the middle line is the  $d = 5$  case, and the bottom line is the  $d = 7$  case. Explicitly, the lines are given by

$$\begin{aligned}
 \omega_I &= 11.16 T & \text{for } d = 4 \\
 \omega_I &= 8.63 T & \text{for } d = 5 \\
 \omega_I &= 5.47 T & \text{for } d = 7
 \end{aligned} \tag{4.2}$$

Notice from Table 1 that as a function of  $r_+$ ,  $\omega_I$  is almost independent of dimension. The

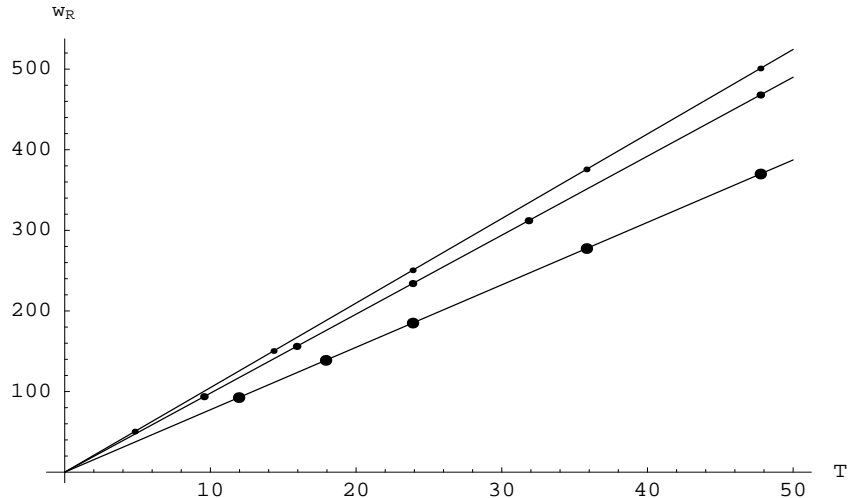


**Fig. 2:** For large black holes,  $\omega_R$  is also proportional to the temperature. The top line is now  $d = 7$ , the middle line is  $d = 5$  and the bottom line is  $d = 4$ .

difference in these slopes is almost entirely due to the dimension dependence of the relation between  $r_+$  and  $T$  (2.10). In contrast,  $\omega_R$  does depend on the dimension, and in fig. 2, the order of the lines is reversed:

$$\begin{aligned}
 \omega_R &= 10.5 T & \text{for } d = 7 \\
 \omega_R &= 9.8 T & \text{for } d = 5 \\
 \omega_R &= 7.75 T & \text{for } d = 4
 \end{aligned}
 \tag{4.3}$$

This linear scaling with the temperature is in agreement with the general argument in section 2. According to the AdS/CFT correspondence,  $\tau = 1/\omega_I$  is the timescale for the approach to thermal equilibrium. Eq. (4.2) is one of the main results of this work.

For the intermediate size black holes, the quasinormal frequencies do not scale with the temperature. This is clearly shown in fig. 3 which plots  $\omega_I$  as a function of  $r_+$  for  $d = 4$  black holes with  $r_+ \sim 1$ . To a remarkable accuracy, the points continue to lie along a straight line  $\omega_I = 2.66 r_+$ . The dashed curve represents the continuation of the curve  $\omega_I = 11.16 T$  shown in fig. 1. to smaller values of  $r_+$ . (For large  $r_+$  these two curves are identical.) It is not yet clear what the significance of this linear relation is for the dual CFT. Some speculations are given in section 6. Since the quasinormal frequencies can be computed to an accuracy much better than the size of the dots in fig. 3, one can check that the points actually lie slightly off the line. This is shown more clearly in the five

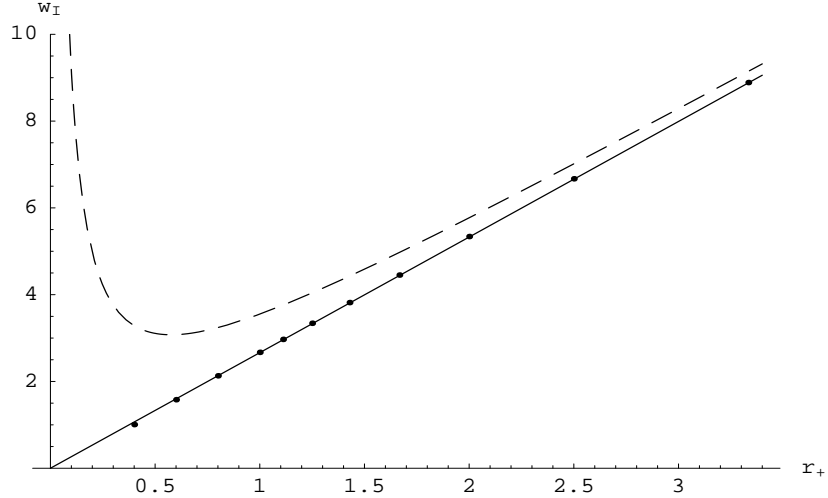


**Fig. 3:**  $\omega_I$  for intermediate black holes in four dimensions. The solid line is  $\omega_I = 2.66 r_+$ , and the dashed line is  $\omega_I = 11.16 T$ .

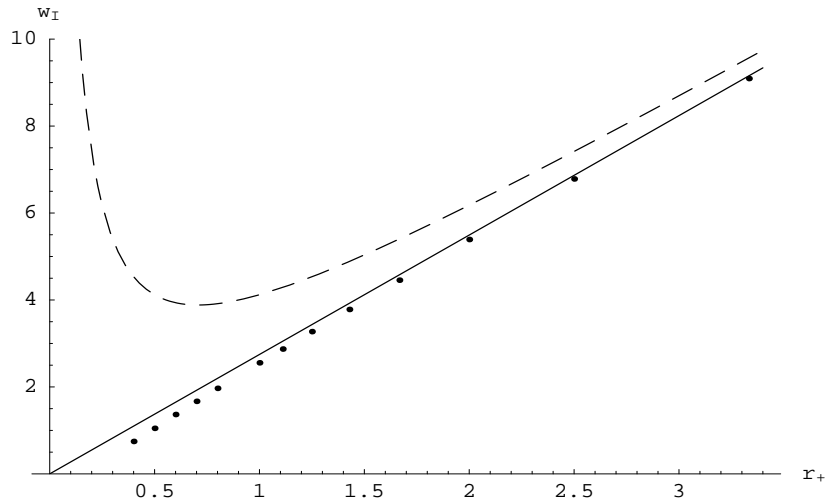


**Fig. 4:**  $\omega_I$  for intermediate black holes in five dimensions. The solid line is  $\omega_I = 2.75 r_+$ , and the dashed line is  $\omega_I = 8.63 T$ .

dimensional results in fig. 4. Once again the dashed curve is the continuation of the curve  $\omega_I = 8.63 T$  shown in fig. 1, and the solid curve is the line  $\omega_I = 2.75 r_+$  that it approaches asymptotically.

The real part of the quasinormal frequencies are shown in similar plots in fig. 5 for  $d = 4$  and fig. 6 for  $d = 5$ .  $\omega_R$  approximates the temperature more closely than the black hole size, but it is clear from fig. 6 that it is not diverging for small black holes.

We have so far discussed only the lowest quasinormal mode with  $l = 0$ . We have also computed higher modes and modes with nonzero angular momentum, but the numerical

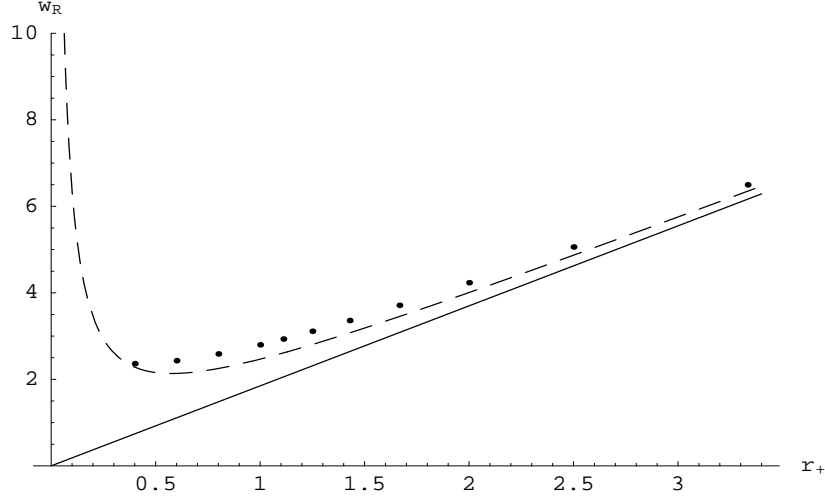


**Fig. 5:**  $\omega_R$  for intermediate black holes in four dimensions. The solid line is  $\omega_R = 1.85 r_+$ , and the dashed line is  $\omega_R = 7.75 T$

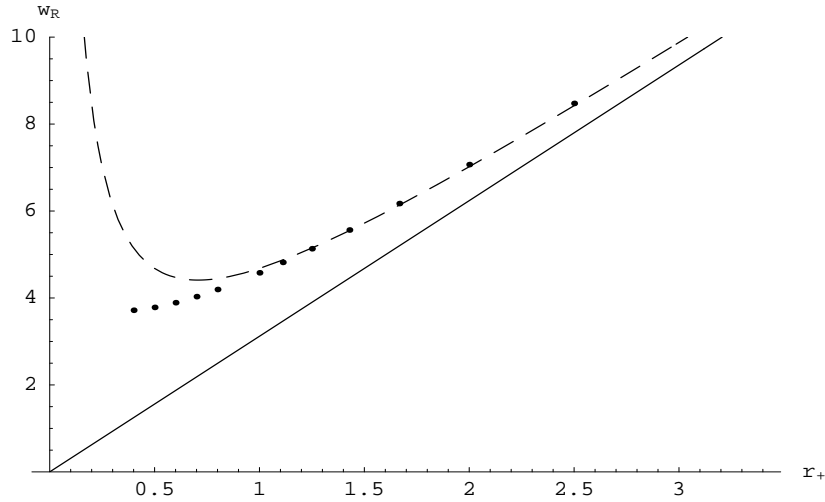


**Fig. 6:**  $\omega_R$  for intermediate black holes in five dimensions. The solid line is  $\omega_R = 3.12 r_+$ , and the dashed line is  $\omega_R = 9.8 T$

accuracy decreases as one increases the mode number  $n$  or  $l$ . So we restrict our attention to relatively small values of  $n$  and  $l$ .

For large black holes, in both four and five dimensions, we find that the low lying quasinormal modes are approximately evenly spaced in  $n$ . In particular, for  $r_+ = 100$ ,  $\omega_I(n) \approx 41 + 225 n$  and  $\omega_R(n) \approx 54 + 131 n$  in four dimensions, whereas  $\omega_I(n) \approx 73 + 201 n$  and  $\omega_R(n) \approx 106 + 202 n$  in five dimensions.

Increasing the angular momentum  $l$  mode has the surprising effect of increasing the damping time scale ( $\omega_I$  decreases), and decreasing the oscillation time scale ( $\omega_R$  increases).



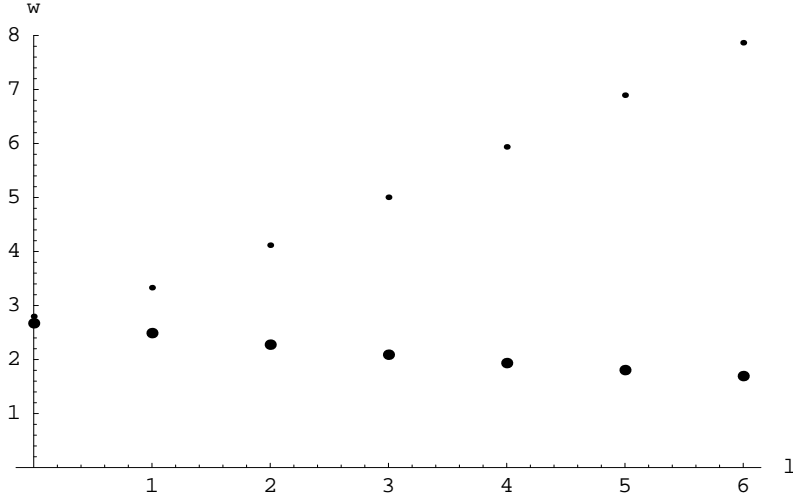


**Fig. 7:** Dependence of  $\omega$  on  $l$  for four dimensional black hole with  $r_+ = 1$ . The smaller points are  $\omega_R$ , the larger points are  $\omega_I$ .

This is shown in fig. 7, where  $\omega_R$  (smaller points) and  $\omega_I$  (larger points) are plotted against  $l$  for low values of  $l$ .<sup>5</sup> An important open question is the behavior of  $\omega_I$  as  $l \rightarrow \infty$ . It appears to decrease with  $l$ , but the general argument in section 2 shows that it cannot become negative. If  $\omega_I$  continues to decrease with  $l$ , then the late time behavior of a general perturbation will be dominated by the largest  $l$  mode. The large  $l$  behavior of  $\omega_I$  is currently under investigation. Preliminary results indicate that the frequencies stay bounded away from zero. If this were not the case, and  $\omega_I$  approached zero fast enough, then a general superposition of all spherical harmonics could decay at late times only as a power law. However, even this would not be a problem for the AdS/CFT correspondence, since the decomposition into spherical harmonics can be done in the boundary field theory as well. The statement is that, e.g., a perturbation of  $\langle F^2 \rangle$  with given angular dependence  $Y_l$  on  $S^3$  will decay exponentially with a time scale given by the imaginary part of the lowest quasinormal mode with that value of  $l$ .

## 5. Comments on small black holes

In this section we briefly discuss the extrapolation of the quasinormal frequencies to the small black hole regime ( $r_+ \ll R$ ). Our numerical approach becomes unreliable in this regime, so we cannot compute them directly. Instead, we must rely on indirect arguments. But first we give some motivation for exploring this question.

---

<sup>5</sup> The size of the dots is not related to the accuracy of the calculation.

Small AdS black holes are not of direct interest for the AdS/CFT correspondence. This is because an extended black hole of the form Schwarzschild-AdS cross  $S^m$  is unstable to forming a black hole localized in all directions whenever the radius of the black hole is smaller than the radius of the sphere. This is a classical instability first discussed by Gregory and Laflamme [16]. It is quite different from the Hawking-Page transition [17,18] which applies to black holes in contact with a heat bath. In that case, when the black hole is of order the AdS radius it undergoes a transition to a thermal gas in AdS. The Hawking-Page transition can be avoided if we consider states of fixed energy, not fixed temperature. Then black holes dominate the entropy even when  $r_+ < R$  and continue to do so until  $r_+/R$  is less than a negative power of  $N$  [19,20]. The situation is very similar to the old studies of a black hole in a box. For fixed total energy, the maximum entropy state consists of most of the energy in the black hole, and a small amount in radiation. Unfortunately, the stable small black hole configuration must be a ten or eleven dimensional black hole (by the Gregory-Laflamme instability) and is not known explicitly.

Nevertheless, there may be other applications of the quasinormal modes of small black holes in AdS. One possibility comes from the striking fact (shown in fig. 3) that for  $d = 4$ ,  $\omega_I$  is proportional to  $r_+$  to high accuracy. As we will discuss below, the slope of this line, 2.66, turns out to be numerically very close to a special frequency which arises in black hole critical phenomena first studied by Choptuik [12]. To explore this possible connection, one needs to consider quasinormal modes of small black holes.

From the intermediate black hole results shown in the previous section, it is tempting to speculate that as  $r_+ \rightarrow 0$ ,  $\omega_I \rightarrow 0$ , and  $\omega_R \rightarrow \text{constant}$ . Since the decay of the field is due to absorption by the black hole, it is intuitively plausible that as the black hole becomes arbitrarily small, the field will no longer decay. It is even possible that the quasinormal modes approach the usual AdS modes in the limit  $r_+ \rightarrow 0$ , although this is not guaranteed since the boundary conditions at  $r = r_+$  do not reduce to regularity at the origin as  $r_+ \rightarrow 0$ . If they do approach the usual modes in this limit, then  $\omega_R$  must approach  $d - 1$  [21]. Of course, in the context of string theory, one cannot trust the Schwarzschild-AdS solution when the curvature at the horizon becomes larger than the string scale. By taking the AdS radius  $R$  sufficiently large, one can certainly use this solution to describe some small black holes, but the geometry would have to be modified before the limit  $r_+ \rightarrow 0$  is reached.

It has been shown that the low energy absorption cross section for massless scalars incident on a general asymptotically flat spherically symmetric black hole is always equal

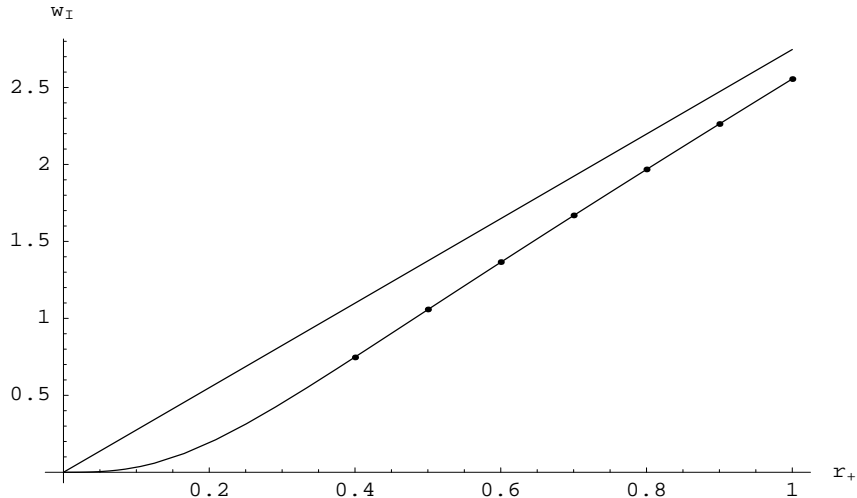


**Fig. 8:** The curved line is a fit to the modes of a small black hole in  $d = 5$ . The modes approach the straight line shown at large  $r_+$ .

to the area of the event horizon [22]. We can use this to estimate the imaginary part of the lowest quasinormal mode for a small AdS black hole as follows. Imagine a wave with energy of order  $1/R$  propagating toward a black hole with  $r_+ \ll R$ . Then the spacetime around the black hole is approximately Schwarzschild, and the low energy condition is satisfied, so the amplitude of the reflected wave  $\Phi_r$  will be reduced from the amplitude of the incident wave  $\Phi_i$ , by  $1 - (\Phi_r/\Phi_i)^2 \sim r_+^{d-2}$ . After a time of order the AdS radius, the reflected wave will bounce off the potential at infinity with no change in amplitude. It will again encounter the black hole potential and be partly absorbed and partly reflected. Repeating this process leads to a gradual decay of the field  $\Phi \sim e^{-\alpha t}$  with  $\alpha \sim r_+^{d-2}$ .

This suggests that for small black holes,  $\omega_I$  should scale like the horizon area  $r_+^{d-2}$ . In the large black hole regime, on the other hand, we know that the modes should scale linearly with  $r_+$ . To check this, we consider a simple ansatz which interpolates between these two regimes and see how well it fits the data. Consider the function  $\omega_I(r_+) = \frac{ar_+^m}{b+r_+^{m-1}}$  (where  $a$  corresponds to the asymptotic slope). For each  $m$  we choose  $b$  to give the best fit to the intermediate black hole data, and see which  $m$  yields the lowest overall error (as measured by  $\chi^2$ ).

In the five dimensional case, using seven points between  $r_+ = .4$  and  $r_+ = 1$ , we indeed find that  $m = 3$  gives the best fit:  $\chi^2 \approx 9 \times 10^{-6}$  for  $m = 3$ , as opposed to  $\chi^2 \approx 3 \times 10^{-2}$  for  $m = 2$  and  $m = 4$ . The actual fit, shown in fig. 8 along with the modes and the asymptotic line, is given by  $\omega_I(r_+) \approx \frac{2.746675r_+^3}{0.0748+r_+^2}$ . In four dimensions the story is much less clear, since there is no significant difference between the fit with  $m = 2$  and the fit with

$m = 3$ . This could be due to the fact that the data for intermediate black holes have not yet started to significantly deviate from a straight line.

To see the possible connection with black hole critical phenomena, consider the evolution of a self gravitating spherically symmetric scalar field (in an asymptotically flat 4d spacetime). It is clear that weak waves will scatter and go off to infinity, just like in flat spacetime. Strong waves will collapse and form a black hole. Choptuik [12] studied one parameter families of initial data (labelled by  $p$ ) which interpolated between these two extremes. In each case there is a critical solution  $p = p_*$  which marks the boundary between forming a black hole or not forming one. The late time behavior of this critical solution turns out to be universal. It has precisely one unstable mode which grows like  $e^{\lambda t}$  with  $\lambda = 2.67$ . This mode is responsible for the famous scaling of the black hole mass for  $p$  just above the critical value,  $M_{bh} \sim (p - p_*)^\gamma$  where  $\gamma = 1/\lambda = .374$ . (For a review, see [23].)

The numerical value of  $\lambda$  is very close to the slope, 2.66, of the line in fig. 3 giving the imaginary part of the quasinormal mode frequencies. Since both numbers involve imaginary frequencies for spherically symmetric scalar fields in four dimensions, it is natural to wonder if there might be a deeper connection between these two phenomena. Unfortunately, it appears at the moment that the agreement is just a numerical coincidence. The first thing one might check is whether the agreement continues in higher dimensions. Although the critical solutions for black hole formation have not been studied in five or seven dimensions, they have recently been calculated in six dimensions [24] with the result  $\lambda = 1/.424 = 2.36$ . We have redone our calculation in six dimensions and do not find agreement. The slope of  $\omega_I$  as a function of  $r_+$  turns out to be 2.693. Another difference is that the exponents in black hole critical phenomena are known to be independent of the mass of the scalar field. We have checked that the quasinormal frequencies of large and intermediate black holes do depend on the mass. One might expect that if there is a connection between these two phenomena, it would apply in the limit of small AdS black holes. However, we have seen that the modes of small black holes actually deviate from the linear relation, so the significance of the asymptotic slope is not clear. While it is still possible that some deeper connection exists (perhaps just in four dimensions and for massless fields) it appears unlikely.

As an aside, we note that if one repeats the calculation of critical phenomena for spacetimes which are asymptotically AdS, the late time results will be quite different. Since energy cannot be lost to infinity, if one forms a black hole at all, it will eventually

grow to absorb all the energy of the initial state.

## 6. Conclusions

We have computed the scalar quasinormal modes of Schwarzschild-AdS black holes in four, five, and seven dimensions. These modes govern the late time decay of a minimally coupled massless scalar field, such as the dilaton. For large black holes, it is easy to see that these modes must scale with the black hole temperature  $T$ . By the AdS/CFT correspondence, this decay translates into a timescale for the approach to thermal equilibrium in the CFT, for large temperatures and perturbations dual to the scalar field. The timescale is simply given by the imaginary part of the lowest quasinormal frequency,  $\tau = 1/\omega_I$ . From (4.2), for perturbations with homogeneous expectation values ( $l = 0$  modes) these timescales are  $\tau = .0896/T$  for the three dimensional CFT,  $\tau = .116/T$  for the four dimensional super Yang-Mills theory, and  $\tau = .183/T$  for the six dimensional  $(0, 2)$  theory. As we mentioned earlier, these time scales are universal in the sense that all scalar fields with the same angular dependence will decay at this rate. Perturbations associated with other linearized supergravity fields will decay at different rates, given by their quasinormal mode frequencies.

Perhaps the most surprising aspect of our analysis are the results for intermediate size black holes. For black holes with size of order the AdS radius, we find that the quasinormal frequencies do not continue to scale with temperature, but rather scale approximately linearly with horizon radius. We do not fully understand the implications of this linear relationship for the dual field theories, but we can make the following comments. If one considers the field theory at constant temperature, and slowly lowers the temperature, then one encounters the Hawking-Page transition [17,18]. At this point the supergravity description changes from the euclidean black hole to a thermal gas in AdS. For these low temperatures, the relaxation time might still scale with the temperature, but it cannot be computed by a classical supergravity calculation, and is not related to quasinormal frequencies.

To interpret the quasinormal frequencies of intermediate size black holes, we must consider a microcanonical description. Consider all states in the CFT with energy equal to the supergravity energy. Most of these states will be macroscopically indistinguishable, in the sense that they will all have the same expectation values of the operators dual to the supergravity fields. If the only nonzero expectation value is the stress energy tensor,

the states are described on the supergravity side by just the black hole. If you perturb one of these CFT states to one which is macroscopically slightly different, it will decay to a typical state with a timescale set by the lowest quasinormal mode. The results in section 4 show that this decay time is determined by the size of the black hole in the supergravity description. Of course the field theory knows about the black hole size since its entropy is given by the black hole area. However the fact that, in this range of energy, the frequency scales linearly with the radius is puzzling.

The fact that the quasinormal frequencies do not continue to scale with temperature is also interesting for the following reason. For a certain range of energies, the supergravity entropy  $S(E)$  is dominated by small (ten or eleven dimensional) black holes<sup>6</sup> [19]. This means that the effective temperature, defined by  $dS/dE = 1/T$ , has the property that it decreases as the energy increases, i.e. the specific heat is negative. By the AdS/CFT correspondence, the same must be true in the dual CFT. (This is not a problem since it applies to only a finite range of energies.) If the quasinormal modes continued to scale with the temperature, then this negative specific heat would have dynamical effects. Instead, we find that the relaxation time increases monotonically with decreasing energy.

### Acknowledgements

It is a pleasure to thank P. Brady, M. Choptuik, S. Hawking, and B. Schmidt for discussions. We also wish to thank the Institute for Theoretical Physics, Santa Barbara where part of this work was done. This work was supported in part by NSF Grants PHY94-07194 and PHY95-07065.

### Appendix: Evaluation of quasinormal modes

As discussed in section 3, in order to find the quasinormal modes, we need to find the zeros of  $\sum_{n=0}^{\infty} a_n(\omega) (-x_+)^n$  in the complex  $\omega$  plane. We compute the quasinormal modes using Mathematica, in the following way. We search for the zeros,  $\omega_N$ , of  $\psi_N(\omega) \equiv \sum_{n=0}^N a_n(\omega) (-x_+)^n$  by looking for the minima of  $|\psi_N|^2$ , and checking that the value at the minimum is zero,  $|\psi_N(\omega_N)|^2 = 0$ . (In practice, there are numerical errors in the computation, so the value at the minimum is instead  $\sim 10^{-14}$ , or smaller.) In order to

---

<sup>6</sup> As we discussed in the previous section, these black holes can be quantum mechanically stable, since they are in equilibrium with their Hawking radiation.

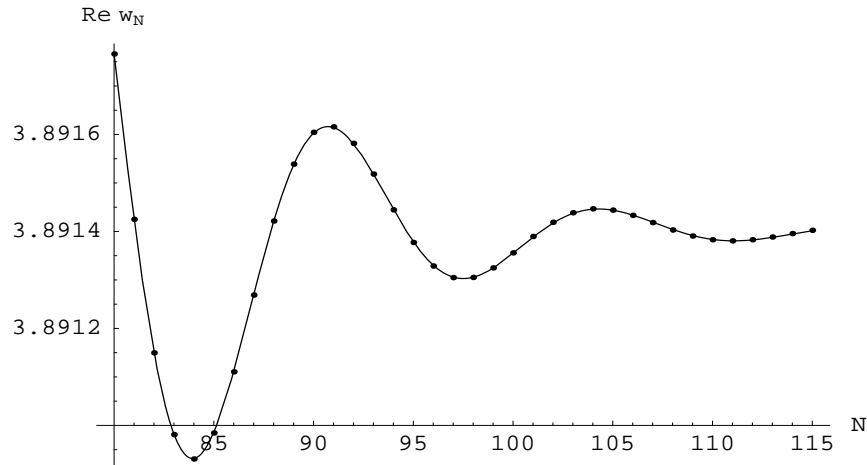


**Fig. 9:** Convergence plot for a five dimensional black hole with  $r_+ = 0.6$

find the correct minimum, we need to specify an initial guess for  $\omega_N$ . (This sometimes poses difficulties in searching for new modes, and apart from using analytical or intuitive understanding as our guide, we are forced to resort to trial and error.) How close to the actual minimum one is required to start depends on the parameters; for the  $n = 1, l = 0$  mode of reasonably-sized black hole, this seldom poses any limitations.

To obtain an accurate estimate of the quasinormal frequencies  $\omega$ , we typically need to compute on the order of  $N = 100$  partial sums, depending on the dimension  $d$ , the black hole size  $r_+$ , and the mode (i.e.  $n$  and  $l$ ). Roughly speaking, at a fixed partial sum  $N$ , the relative error in the computed quasinormal frequency grows as  $r_+$  decreases, and as  $l, n$ , or  $d$  increases.

The task of determining the mode to the necessary accuracy is fortuitously simplified by the fact that the “convergence curve” has a surprisingly simple form. In particular, once the partial sums have converged to sufficient accuracy, the variation of  $\omega_N$  is given by an exponentially damped sine as a function of  $N$ , i.e.  $\omega_N \sim \omega + c e^{-N/a} \sin(bN + d)$  where  $a$  and  $b$  depend on the physical parameters such as  $r_+$ , while  $c$  and  $d$  just depend on which partial sum we start with. In fact, we can use a fitting algorithm in Mathematica to fit these convergence curves. An example is given in fig. 9, where the dots represent  $Re(\omega_N)$  for a particular set of parameters ( $d = 5, r_+ = 0.6, n = 1$ , and  $l = 0$ ), and the solid curve is the corresponding fit. This simplification allows us to determine the mode with a much higher accuracy than we would be led to expect from the spread of  $\omega_N$ . It also allows us to confirm that the numerical errors in the computation of each  $\omega_N$  are negligible, since

otherwise, one would expect a more noisy distribution.

Often the quickest way to obtain the quasinormal mode is to simply look for the minimum of  $|\psi_N|^2$  near various initial guesses for the frequency, but when that method fails, we can also adopt a more systematic approach; eliminating the possibility of occurrence of quasinormal modes in a given frequency range. This may be carried out in a more systematic manner due to the fact that  $Re(\psi_N(\omega))$  and  $Im(\psi_N(\omega))$  are conjugate harmonic functions of  $\omega$ , which must satisfy the maximum principle. Thus, if we find that  $\psi_N(\omega)$  is bounded inside a given region of the complex  $\omega$  plane, and either  $Re(\psi_N(\omega))$  or  $Im(\psi_N(\omega))$  remains nonzero everywhere on the boundary, then  $\psi_N$  is necessarily nonzero everywhere inside that region. This ensures that there can be no quasinormal modes with these frequencies. We can thus systematically search for the lowest modes by eliminating the low frequency regions until we find the modes.

Once we find one mode for a given set of parameters, continuity of the solution allows us to trace the mode through the parameter space; that is, we can find  $\omega$  for nearby values of  $r_+$  and  $l$ . Also, once we know the  $n = 1$  and  $n = 2$  modes for a fixed  $r_+$  and  $l$ , the equal spacing between the modes allows us to find the higher  $n$  modes (provided the numerical errors stay small).

Thus, the procedure for finding  $\omega(r_+)$  is the following: We first consider a large black hole, where the convergence is good at a low partial sum, e.g.  $N = 40$ . For such a low cut-off  $N$  on the partial sum, we may easily compute  $\psi_N(\omega, r_+, l)$  in full generality. We find the desired mode  $\omega_N(r_+, n, l)$  using the method described above, and we can check the convergence by comparing this result with that obtained for the lower partial sums. We can now follow the mode to smaller values of  $r_+$ , until the convergence becomes too slow, and we need to compute higher partial sums. It becomes more practical at this point to fix all the parameters, and consider  $\psi_N$  as a function of  $\omega$  only. This has the numerical advantage of enabling us to compute the partial sums to much higher  $N$ ; the drawback, of course, is that now we need to recompute the whole series for each  $r_+$ .

**Note added:**

After this work was submitted, we have extended our computations of the higher  $l$  modes for large black holes, up to  $l = 25$ . From fits of the large  $l$  behavior of  $\omega_I$ , we find strong evidence that the frequencies indeed stay bounded away from zero: In particular, a fit of the form  $\omega_I(l) = 1.12 + \frac{15.4}{l+11.8}$  has  $\chi^2 \approx 2 \times 10^{-6}$ , as opposed to  $\chi^2 \approx 10^{-3}$  for a fit with  $\omega_I(l \rightarrow \infty) \rightarrow 0$ .



## References

- [1] The earliest papers include C. Vishveshwara, Phys. Rev. D1 (1970) 2870; W. Press, Ap. J. Lett. 170 (1971) L105. For an early review, see S. Detweiler, in *Sources of Gravitational Radiation*, L. Smarr, ed., Cambridge U. Press (1979) p. 221.
- [2] For a recent review, see K. Kokkotas and B. Schmidt, “Quasi-normal modes of stars and black holes”, to appear in Living Reviews in Relativity: [www.livingreviews.org](http://www.livingreviews.org) (1999).
- [3] P. Brady, C. Chambers, W. Krivan and P. Laguna, Phys. Rev. D55 (1997) 7538, gr-qc/9611056; P. Brady, C. Chambers, W. Laarakkers, and E. Poisson, Phys. Rev. D60 (1999) 064003, gr-qc/9902010.
- [4] A. Barreto and M. Zwozski, Math. Research Lett. 4 (1997) 103.
- [5] J. Maldacena, Adv. Theor. Math. Phys. 2 (1998) 231, hep-th/9711200.
- [6] E. Witten, Adv. Theor. Math. Phys. 2 (1998) 253, hep-th/9802150.
- [7] S. Gubser, I. Klebanov, and A. Polyakov, Phys. Lett. B428 (1998) 105, hep-th/9802109.
- [8] For a comprehensive review, see O. Aharony, S.S. Gubser, J. Maldacena, H. Ooguri, and Y. Oz, “Large N Field Theories, String Theory and Gravity”, hep-th/9905111.
- [9] S. Kalyana Rama and B. Sathiapalan, “On the role of chaos in the AdS/CFT connection”, hep-th/9905219.
- [10] J. Chan and R. Mann, Phys. Rev. D55 (1997) 7546, gr-qc/9612026; Phys. Rev. D59 (1999) 064025.
- [11] R. Price, Phys. Rev. D5 (1972) 2419, 2439.
- [12] M. Choptuik, Phys. Rev. Lett. 70 (1993) 9.
- [13] C. Csaki, H. Ooguri, Y. Oz, and J. Terning, JHEP 01 (1999) 017, hep-th/9806021; R. de Mello Koch, A. Jevicki, M. Mihailescu, and J.P. Nunes, Phys. Rev. D58 (1998) 105009, hep-th/9806125; M. Zyskin, Phys. Lett. B439 (1998) 373, hep-th/9806128.
- [14] E.S.C. Ching, P.T. Leung, W.M. Suen, and K. Young, Phys. Rev. D52 (1995) 2118, gr-qc/9507035.
- [15] C. Gundlach, R. Price, and J. Pullin, Phys. Rev. D49 (1994) 883.
- [16] R. Gregory and R. Laflamme, Phys. Rev. Lett. 70 (1993) 2837, hep-th/9301052; Nucl. Phys. B428 (1994) 399, hep-th/9404071.
- [17] S. Hawking and D. Page, Commun. Math. Phys. 87 (1983) 577.
- [18] E. Witten, Adv. Theor. Math. Phys. 2 (1998) 505, hep-th/9803131.
- [19] T. Banks, M. Douglas, G. Horowitz, and E. Martinec, “AdS Dynamics from Conformal Field Theory”, hep-th/9808016.
- [20] G. Horowitz, talk at Strings '99, Potsdam, Germany, to appear in the proceedings.
- [21] C. Burgess and C. Lutken, Phys. Lett. 153B (1985) 137.

- [22] S. R. Das, G. Gibbons, and S. D. Mathur, Phys. Rev. Lett. 78 (1997) 417, hep-th/9609052.
- [23] C. Gundlach, Adv. Theor. Math. Phys. 2 (1998) 1, gr-qc/9712084.
- [24] D. Garfinkle, C. Cutler, and G. C. Duncan, gr-qc/9908044.